



# Initiation-development modelling of allelic losses on chromosome 9 in multifocal bladder cancer

J. Louhelainen <sup>a,\*</sup>, H. Wijkström <sup>b</sup>, K. Hemminki <sup>a</sup>

<sup>a</sup>Center for Nutrition and Toxicology, Karolinska Institute, 141 57 Huddinge, Sweden

<sup>b</sup>Department of Urology, Karolinska Institute, Huddinge Hospital, 141 86 Huddinge, Sweden

Received 23 November 1999; received in revised form 17 February 2000; accepted 25 February 2000

## Abstract

Multiple low-grade, low-stage superficial tumours were analysed for loss of heterozygosity (LOH) on chromosome 9 with 29 markers. Three consensus regions were found, one at 9p (9p21-22) and two at 9q (9q21-31 and 9q32-34). Phylogenetic trees were calculated for each patient using both designated chromosome 9 regions and, separately, using individual microsatellite data. Regional analysis suggested that multiple, equally important regions for bladder tumour initiation exist on chromosome 9. During the development of tumours all regions were eventually affected. The phylogenetic analyses with individual markers were used as molecular clocks to trace the ordering of tumours. The results were compared with the physical locations of the tumours and a hypothetical development model was built. These are novel approaches which, to our knowledge, have not been used before. © 2000 Elsevier Science Ltd. All rights reserved.

**Keywords:** Bladder neoplasms; Loss of heterozygosity; Multifocal tumour; Tumour suppressor gene

## 1. Introduction

Molecular pathology of bladder cancers shows large heterogeneity including loss of heterozygosity (LOH) and deletions in many, if not most, chromosomes. LOH has been found on chromosomes 1p, 1q, 2q, 3p, 4p, 5q, 5p, 7, 8p, 9p, 9q, 10q, 11p, 11q, 13q, 14q, 17p, 18q, 21q and Y (for review see [1]). It has also been shown that genetic instability increases in the pTa→pT1 transition [2]. Evidence from several studies points to the involvement of chromosome 9 in bladder cancer, for reviews see [3,4]. The *p16* tumour suppressor gene at 9p21 is a candidate gene for involvement in the development of bladder cancer. Homozygous deletions of *p16* have been demonstrated both in primary tumours and in cell lines [5–9]. Preneoplastic changes of the bladder epithelium or superficial tumours sometimes precede malignancy but the patients do not always develop bladder cancer [10–13]. The aim of our study was to characterise the

sequential allelic losses at chromosome 9 by means of a microsatellite analysis. To eliminate the genetic heterogeneity and phenotype problems typical of bladder cancer we chose patients with multifocal tumours. Analysis of changes seen in an identical genetic background should reveal the key genetic events during development. These tumours are clonally related, which makes it possible to arrange them in chronological order [14]. We investigated multifocal tumours with surrounding tissues from 5 patients using 29 microsatellite markers covering chromosome 9. Blood samples were used as references since normal bladder mucosa is known to have genetic alterations. Phylogenetic-type analyses were performed to pinpoint the early changes on chromosome 9. We also modelled the spreading of tumours by superimposing genetic and pathology data.

## 2. Materials and methods

Tumours, visually normal mucosal tissue and blood was collected from 5 patients with superficial, multifocal bladder cancer (Table 1). All the tumours were recur-

\* Corresponding author. Tel.: +46-8-6089242; fax: +46-8-6081501.

E-mail address: jarlo@thon.csb.ki.se (J. Louhelainen).

rent and of the transitional cell type. No treatment other than transurethral resections had been attempted before. All tumours were resected transurethrally and each tumour sample was separated into two halves. One half was sent for routine histopathological examination and the other half immediately frozen in liquid nitrogen. Biopsies (2 mm in size) from macroscopically normal bladder mucosa, adjacent to each tumour, were handled in the same manner.

Polymerase chain reaction (PCR) was performed using Perkin-Elmer DNA Cycler 480 or MJ Research PTC-200 in a 5 µl reaction volume and the reaction products were analysed with an Applied Biosystems 377 or with Pharmacia Alfexpress automatic sequencer. The LOH analysis was performed primarily as previously described [15]. LOH was defined as a reduction of at least 30% of the signal compared with the normal tissue DNA allele. For calculations the following formula was used:  $L = T1:T2/N1:N2$  when  $L < 1$ , or  $1 / (T1:T2/N1:N2)$  if  $L \geq 1$ , where  $T1$ ,  $T2$  = intensity of tumour alleles;  $N1$ ,  $N2$  = intensity of normal tissue alleles;  $L$  = LOH ratio. Allelic imbalances were rare. The marker 1AJL is an intragenic marker for the patched *PTCH* (human homologue of *Drosophila* patched) tumour suppressor gene [16].

We have made two assumptions in the tumour development analysis: (1) loss of heterozygosity correlates with tumour development. During tumorigenesis, the rate of LOH increases which could depend on mutations in other cancer-related genes [17]. (2) The 'spreading' of loss of heterozygosity of specific loci from tumour tissue to surrounding tissue correlates with the tumour development. Earliest genetic changes may be found from preneoplastic lesions hidden in surrounding tissue which are still clinically judged as normal tissue. Studies using the first assumption have been published previously [18–20].

The Camin–Sokal parsimony method used in constructing phylogenetic trees explains the data by assuming that changes  $0 \rightarrow 1$  are allowed but not changes  $1 \rightarrow 0$ . In this context the change is the non-reversible loss of heterozygosity. The phylogenetic analysis resembles the method, which Kerangueven and colleagues used for single primary tumours [21]. In our study, each tree consists of only samples from 1 patient. This enables us to utilise the individual microsatellite marker data when calculating the phylogeny, since the hetero/homozygosity (excluding LOH) data are constant for each patient. We have demonstrated earlier that these tumours are of monoclonal origin [14]. Thus, the microsatellite allele pattern is identical between different samples of a given patient and LOH at individual markers can be used instead of chromosomal regions. The detected allelic losses should correlate with the tumour development.

The phylogenetic analysis was carried out by using the PAUP\* 4.02b and MacClade 3.08a-software packa-

ges [22,23]. These programs were run on a PowerPC platform (MacIntosh G3/450 MHz). To improve the statistical significance and accuracy, bootstrapping with 1000 replicates and resampling with a random seed were used. Heuristic search was chosen to find the consensus groups fulfilling the 50% majority rule. The best trees were plotted as phylogenetic trees, i.e. phylo- or cladograms. In these trees the time flow is unidirectional, moving from top to bottom. The samples are grouped in terms of LOH patterns that indicate common ancestors. All of the descendants above a branch point share that new LOH at the specific loci; none of the samples past this point does.

First, individual marker data were used to calculate the phylogenetic trees. These trees were plotted as cladograms, where all branches have the same height. They were constructed so that they showed only microsatellite markers with unambiguous changes. The model for ordering of the tumours is based on these cladograms — primarily the order of tumours and secondarily the order of the surrounding tissue samples. In the second part, four chromosomal regions were selected for chromosome region analysis. The aim was to select regions, which seem to have importance during initiation (judged from the cladograms) and coincide with minimal deletions and LOH maximums. To illustrate the stepwise changes the results with these four regions were plotted as phylograms, where the branch length is proportional to the number of changes in that branch.

### 3. Results

Twenty-nine markers were analysed on chromosome 9. The microsatellite map of chromosome 9 is shown in Fig. 1. In total 72 samples of tumour tissues, surrounding

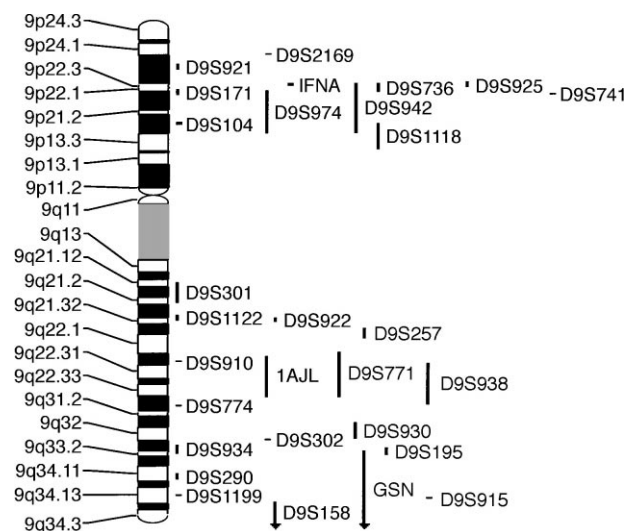


Fig. 1. Microsatellite markers used to detect loss of heterozygosity (LOH).

tissues and blood were collected from 5 patients, each having 2–11 tumours (Table 1). All tumours were non-invasive and of low grade (G1–G2). The LOH patterns are illustrated in Fig. 2, and the LOH results for chromosome 9 are shown in Fig. 3. Most of the tumours (T) have large regions with LOH. The surrounding tissue (N) display only a few changes, thus giving higher resolution for the LOH analysis. The minimal deletions were compared, and at least three consensus deletions could be resolved (Fig. 4). These regions are indicated by both tumour and surrounding tissues. The first region consisted of markers from D9S741 to D9S942 (9p21–22). D9S942 (closest to the *p16* gene) and three adjacent markers telomeric to it formed this consensus region, and all of these four markers were included in 60% (3/5) of the minimal deletions. This consensus region had three tumour LOH maximums (threshold 75%) and two surrounding tissue LOH maximums (threshold 25%). Both the tumours and surrounding tissues have a LOH maximum at D9S741, which is telomeric to *p16*. One of the tumour LOH maximums is near *p16* at D9S942. The second consensus region spans from D9S257 to D9S774 (9q21–31). The *PTCH* marker (1AJL) and three adjacent markers to it were included in 80% (4/5) of the minimal deletions of the tumour samples. The D9S257 marker centromeric to *PTCH* belong to 60% (3/5) of the minimal deletions of the surrounding samples. The third region was from D9S195 to D9S915 (9q32–34). One of the markers (D9S1199 at 9q34) was included in the minimal dele-

tions of all the samples analysed, and four other markers surrounding it were included in 80% (4/5) of the minimal deletions. Three tumour LOH maximums were evenly distributed over this region whereas the surrounding LOH maximum ( $n=1$ ) was biased towards the telomere.

Using chromosomal regions in phylogenetic-type analysis equalises the individual hetero/homozygosity patterns so that the phylogenetic trees are comparable with each other. For modelling purposes we divided chromosome 9 into four regions, each consisting of 4–6 microsatellite markers. Selection of regions was based on the individual marker-based phylogenetic trees, minimal deletions and LOH maximums. Our aim was to select markers, which were chronologically early, included in the minimal deletions and had a high overall LOH rate. These regions (9p21–22, 9q21–q22, 9q22–q32 and 9q33–34) are shown in Fig. 4 (panel 3). The consensus deletion at 9q21–22 was split in two regions because the LOH maximums of surrounding and tumour samples did not align (Fig. 4, panel 2). Only the branches leading to tumours were taken into account

Table 1  
Clinical details of the patients studied<sup>a</sup>

Patient	Total no. of samples	Sex	Sample code	Tissue	Stage	Grade
1	4	M	T1	Tumour	Ta	–
			N1	Mucosa	–	–
			T2	Tumour	Ta	G1
			N2	Mucosa	–	–
2	13	M	T1–T6	Tumour	Ta	G1
			N1–N6	Mucosa	–	–
			T7	Tumour	Ta	G2
3	21	M	N1–N11	Mucosa	–	–
			T1–T11	Tumour	Ta	G2
4	21	M	N1.1–N9	Mucosa	–	–
			T1–T9	Tumour	Ta	G2
5	8	M	N1–N4	Mucosa	–	–
			T1–T4	Tumour	Ta	G2

<sup>a</sup> In addition at least one blood sample per patient were analysed as a reference.

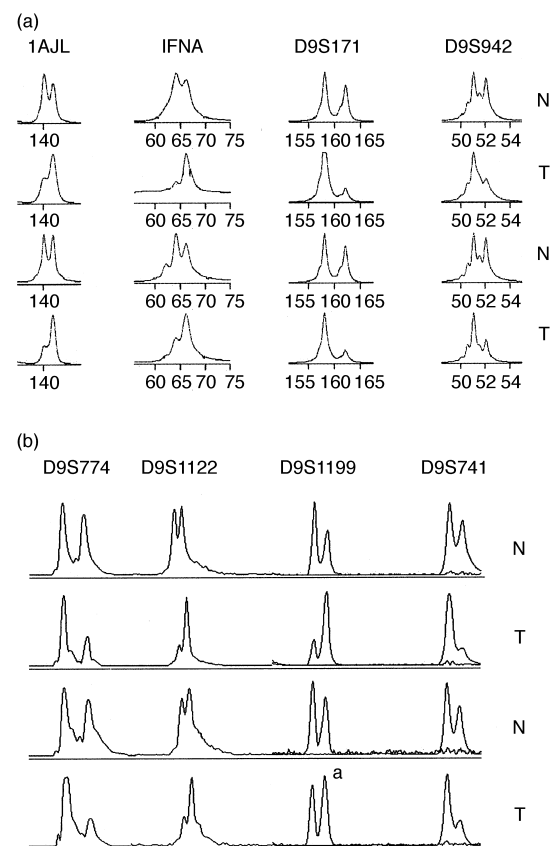


Fig. 2. LOH patterns of microsatellite markers. N, surrounding tissue; T, tumour tissue. Panel A electropherograms are from Pharmacia Alflexpress and panel B results from Applied Biosystems 377. All the tumour samples shown here were judged as LOH, except the D9S1199 lower tumour<sup>a</sup> in panel B.

(Fig. 5). The initiation-development models based on the phylogenetic-type analysis (with the chromosomal regions) are illustrated in Fig. 6. These results suggest that regions 1 (9p21-22), 2 (9q21-q22) and 4 (9q33-34) are equally important for initiation, and region 3 (9q22-32) is involved in later events. According to our model, patients 1 and 2 have an initiation point at region 4, patients 4 and 5 at region 2 and patient 3 at region 1.

We performed modelling of bladder cancer development using emerging LOH as a marker of genetic events. Only changes from heterozygosity to allelic loss were allowed (irreversible changes, also known as 'Camin-Sokal' parsimony). The samples near the roots of the tree represent the samples with least changes (LOH) and the tops of the trees have the highest number of changes. Thus, the top of the tree represent the first tumours in a given urinary bladder, whereas the tumours near the root of the tree are considered the

latest. Surrounding tissue samples accumulate near the roots of the trees since they tend to have fewer changes than the tumours. Both individual marker data and clustered analysis of the four regions were used. The individual marker approach can be used as a molecular clock for the tumorigenesis of a given patient, whereas the chromosomal region analysis allows the comparison of patients. The results of the regional analysis were drawn as phylograms (Fig. 5). Phylogenetic trees based on individual microsatellite markers can be used as a molecular clock to arrange the samples in a chronological order. This approach takes account of all the allelic losses and arranges the samples using the irreversible LOH assumption. Phylogenetic trees based on individual marker data are shown in Figs. 7 and 8. In general, tumours are clustered together having the shared allelic loss at specific microsatellite marker(s) near the root of the tree. These trees are not comparable

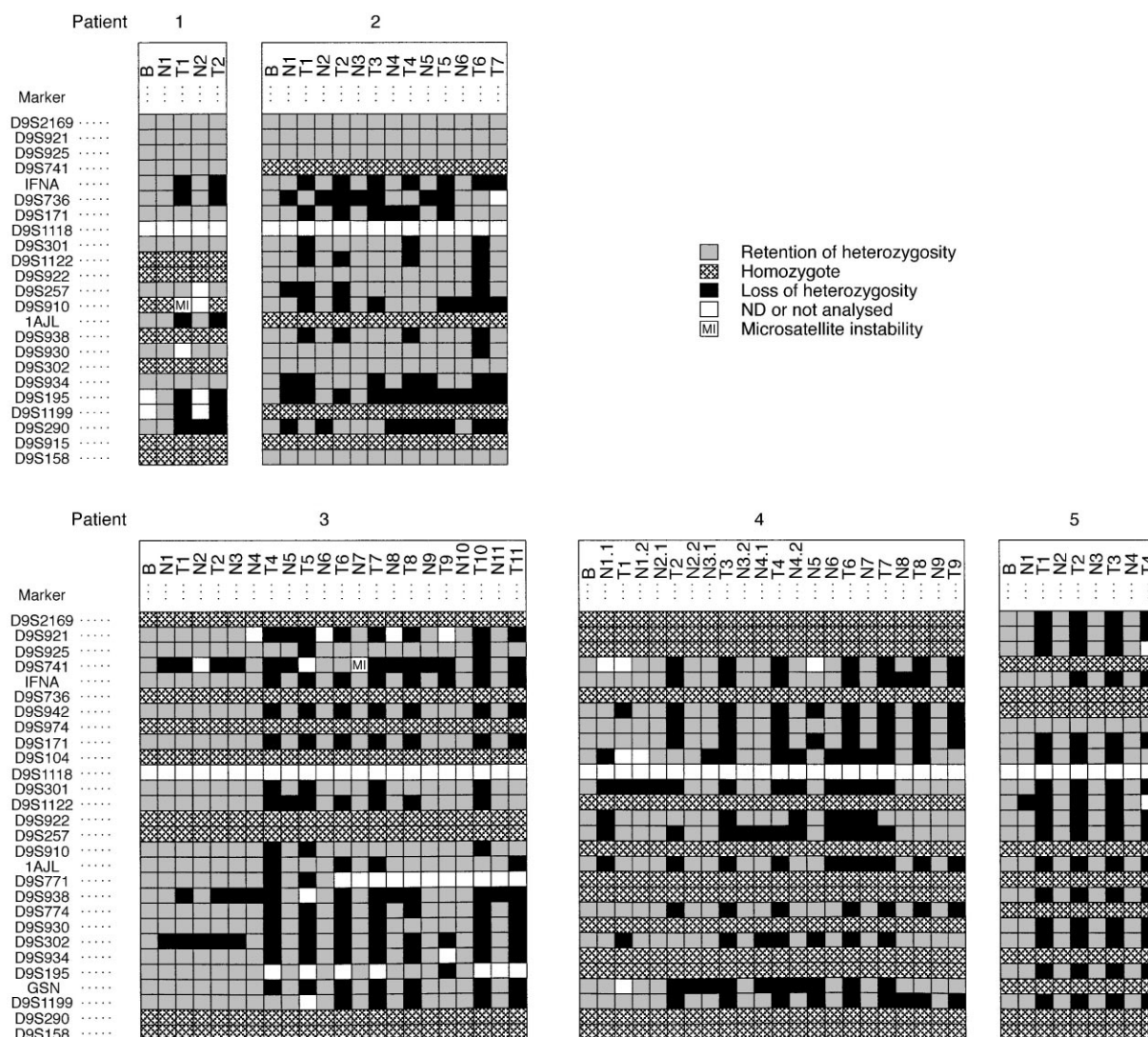


Fig. 3. Loss of heterozygosity of the 5 patients analysed. T, tumour; N, surround; B, blood.

with each other, since the hetero/homozygosity pattern is unique for each patient, i.e. a marker which is heterozygote for 1 patient, can be homozygote for another and vice versa. We scored the samples according to these results and used the pathological information to build a histological development model for each patient (Fig. 9). The arrows indicate the direction of development from the physiologically oldest tumours to the youngest. The chromosomal changes of a given patient should be roughly time dependent since the grade and stage is identical between the patient's tumours.

#### 4. Discussion

The role of chromosome 9 has been the focus of bladder cancer research for several years [3,4]. Monosomy 9 was one of the first anomalies found in several cytogenetic studies [24–27]. Monosomy has usually been interpreted to mean that at least one tumour suppressor gene is present in both chromosome arms. However, van Tilborg and associates recently reported that true monosomy is rare in bladder cancer [28]. The early LOH studies suggested the presence of at least one tumour suppressor gene on chromosome 9 [29–31]. The first attempts to map chromosome 9 pinpointed the regions between 9p12 and 9q34.1 [32] and between 9p12-13 and 9q22 as being important [33]. In more recent studies, multiple candidate regions have been discovered [34–38]. All in all, chromosome 9 seems to

harbour at least four tumour suppressor genes [39]. One of the suggested candidate genes is *DBCCR1* at 9q32-q33, which was found and characterised quite recently [40,41].

Evidence for divided LOH distributions on chromosome 9 have been seen in some studies. Orlow and associates [35] found associations between 9q abnormalities with Ta lesions and both 9q and 9p abnormalities with T1 lesions whereas Simoneau and colleagues [42] could divide their patients into two groups using the LOH pattern on 9q but could not distinguish if tumour formation is initiated by 9q or 9p alterations.

In urinary bladder cancer, two novel tumour suppressor genes proximal and distal to the *p16* gene were recently identified [43]. In our hands, one frequently deleted area at 9p spans the *p16* location but the peak of the affected region in 9p (9p21-22) seems to be shifted slightly to the telomeric side of the *p16* gene. The marker D9S741 had a local LOH maximum both in tumour and surrounding samples. Interestingly, Baud and colleagues found that 50% of the normal mucosa samples had LOH at D9S156, which is located at 9p23-22 [11]. They suggested that the marker D9S156 could be a fragile site or an indicator of bladder epithelium impairment, rather than a tumour initiation marker. Actually, inside our first consensus deletion (Fig. 4, panel 2) our LOH maximums are split in two halves: the first one at D9741 and the second one at D9S736 and D9S942. The D9S736/D9S942 markers are near to the *p16* tumour suppressor gene, whereas D9S741 is closer to the marker D9S156 used by Baud and colleagues. This division could be due to the D9S156 region although there is no concrete evidence to support this. However, patient 3 has a subset of 'normal' samples with allelic loss at D9S471 in Fig. 7. The long arm of chromosome 9 is known to encompass several tumour suppressor genes, but none of the known genes have been clearly implicated in bladder cancer. The first 9q region we resolved involves an intragenic microsatellite marker for the *PTCH* (9q22.3) tumour suppressor gene. When we also analysed the surrounding tissues, the region near *PTCH* was split so that the two adjacent tumour LOH maximums (at D9S938, D9S774) were telomeric to *PTCH* but the surrounding LOH peak was centromeric to the *PTCH* gene (at D9S910). The third region in 9q we could resolve maps to 9q33-34. It remains to be seen if 9q32-34 region contains only one or several tumour suppressor genes important in bladder cancer. However, it is worth considering that the order of the microsatellite markers in the 9q region has been controversial since the YAC clones near or at this region are apparently prone to rearrangements and/or deletions [44].

Modelling of bladder cancer development has proved to be difficult. To date, the most common approach has

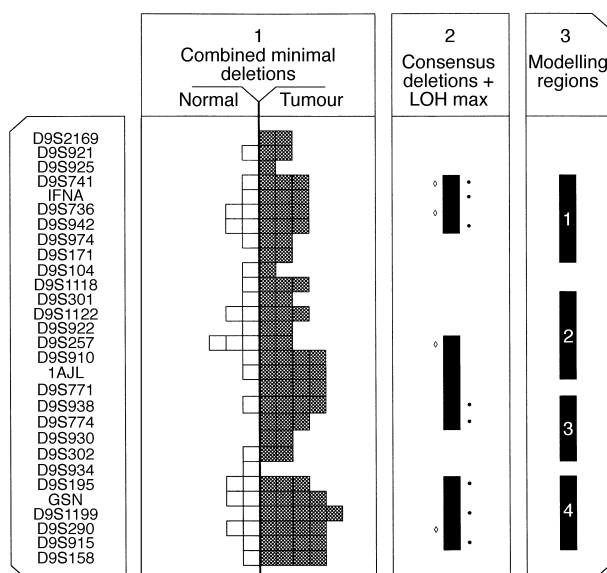


Fig. 4. Panel 1 shows the combined minimal deletions. Panel 2 consensus (N, T) deletions with total LOH maximums, N, hollow markers (threshold 25%); T, solid dots (threshold = 75%). Panel 3 contains the regions used in phylogenetic analysis.

been the analysis of single tumours from each patient and the pooling of the LOH results of all the patients. For a heterogeneous malignancy like bladder cancer this approach might 'dilute' the results so that individual pathways or even initiation cannot be resolved. Recently, Takahashi and associates [20] published a report where they analysed multifocal tumour samples for accumulating allelic loss. They constructed a hypothetical allelic loss model for two patients. For the first patient, the pathway was branched after initiation at 9p/9q and for the second patient, the initiation took place at 9q. In the present study, we tried to push this analysis further by utilising multifocal tumour samples and their

surrounding tissues to reduce heterogeneity and to detect premalignant changes. Multiple markers on chromosome 9 and heuristical phylogenetic-type analysis were used to enhance the resolution. Both individual marker data and clustered analysis of four regions were applied. The first approach can be used as a molecular clock for the tumorigenesis of a given patient, whereas the latter analysis enables the comparison of patients. We can follow the development of individual patients with the method described here and build individual models for each patient. All in all, the tumours analysed arranged into trees, which had only few side branches. Our model suggests that after initiation at a specific

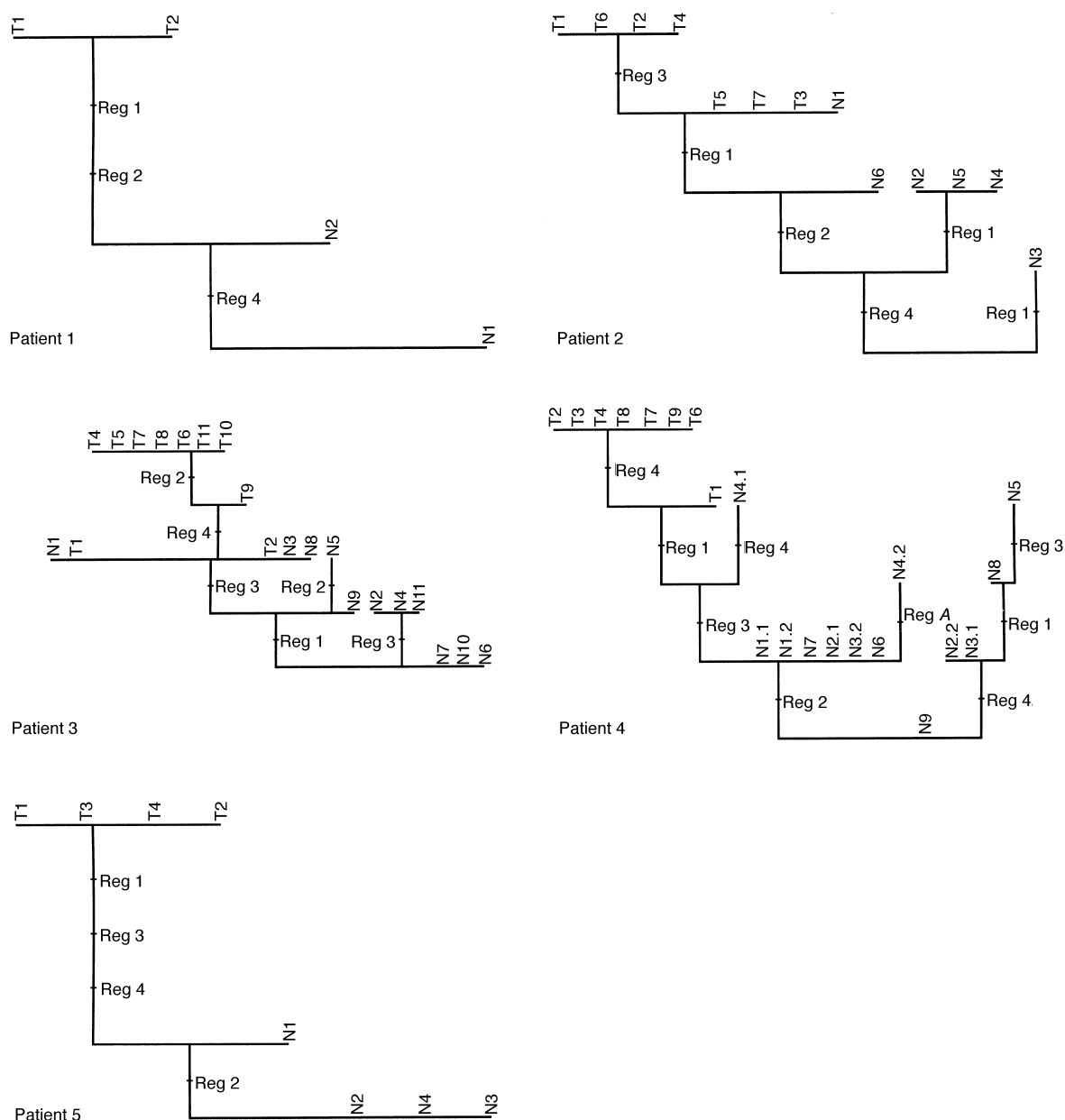


Fig. 5. Cladogram showing the results of the regional analysis. Region 1, 9p21-22; Region 2, 9q21-22; Region 3, 9q22-32; and Region 4, 9q33-34.

locus (9p21-22, 9q21-22 or 9q33-34), the LOH ‘spreads’ to other loci on chromosome 9 leading to a situation where all these regions have lost genetic material (Fig. 6). The results suggest that any of these regions can be involved in the initiation process. Large regions of LOH are usually interpreted as inactivation of multiple tumour suppressor genes. The model presented in Fig. 6

illustrates also the development of chromosomal loss. Our data suggest that most likely at least two hits are needed but are not always sufficient for tumour formation (Fig. 5, patients 2 and 4). It appears that the bladder mucosa often display allelic loss but they are not always tumour-related. This can be seen from the phylo/cladograms where surrounding tissue clusters form side

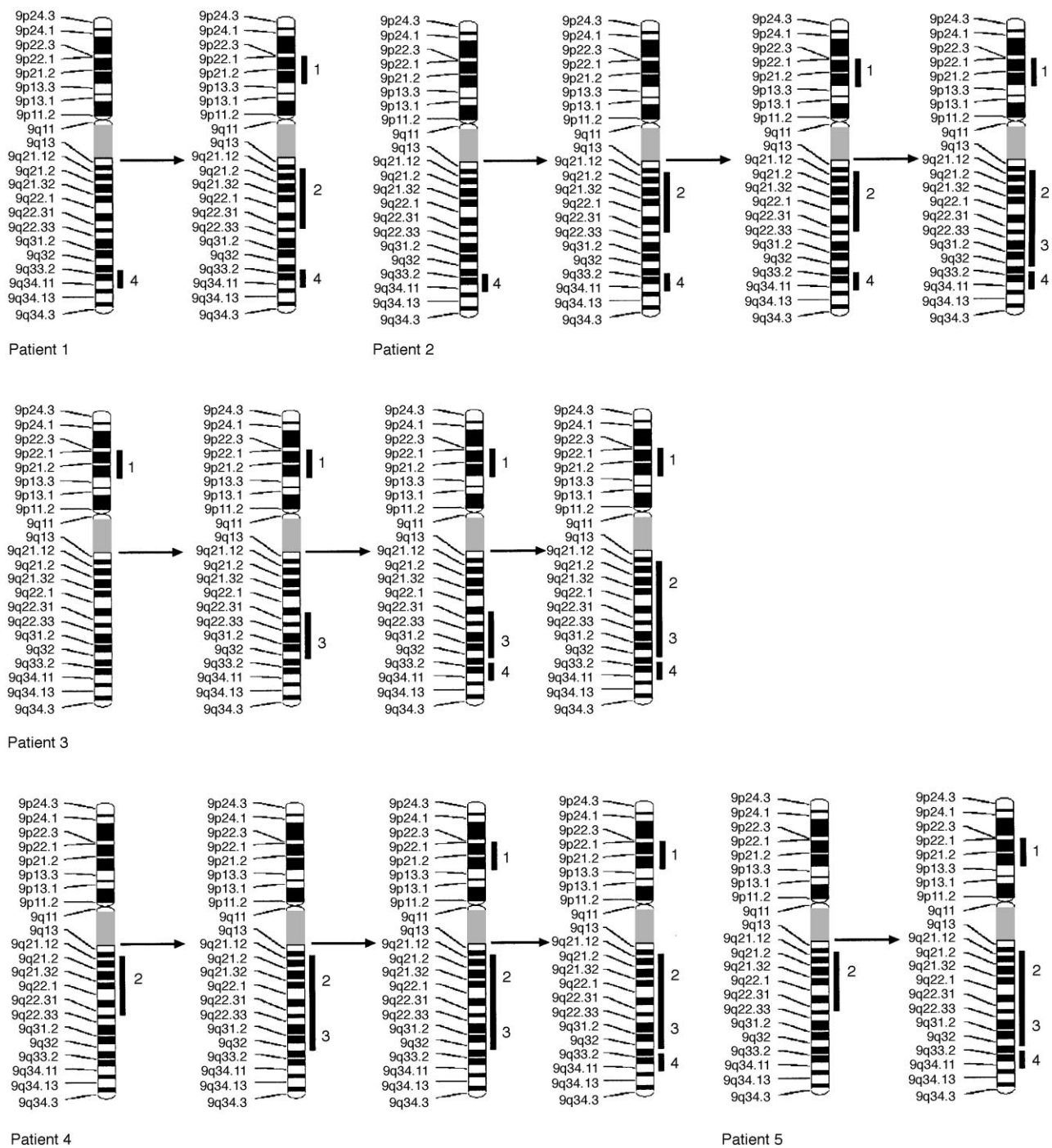


Fig. 6. Initiation-progression model of 5 bladder cancer patients with multifocal tumours based on the regional phylogenetic analysis. Regions 1–4 are marked as black bars next to the ideograms.



Fig. 7. The results of the phylogenetic analysis of patients 1, 2 and 3 using individual microsatellite markers. These data were used for the ordering of tumours.



patient 1 for example does not have any tumours near the trigone vesicular. The model introduced here is a simplified model, and does not take into account the three-dimensional structure of the urinary bladder.

Phylogenetic-type analysis of microsatellite data can help to solve complex genetic problems, to find both common changes and chronological events. In conclusion, this study demonstrates that recurrent multifocal tumour analysis, together with surrounding tissues can help to map the individual development of apparently heterogeneous tumours. We could follow the initiation-development of a given patient. The result suggests that three regions are important during initiation but the development pathway at chromosome 9 varies in each individual.

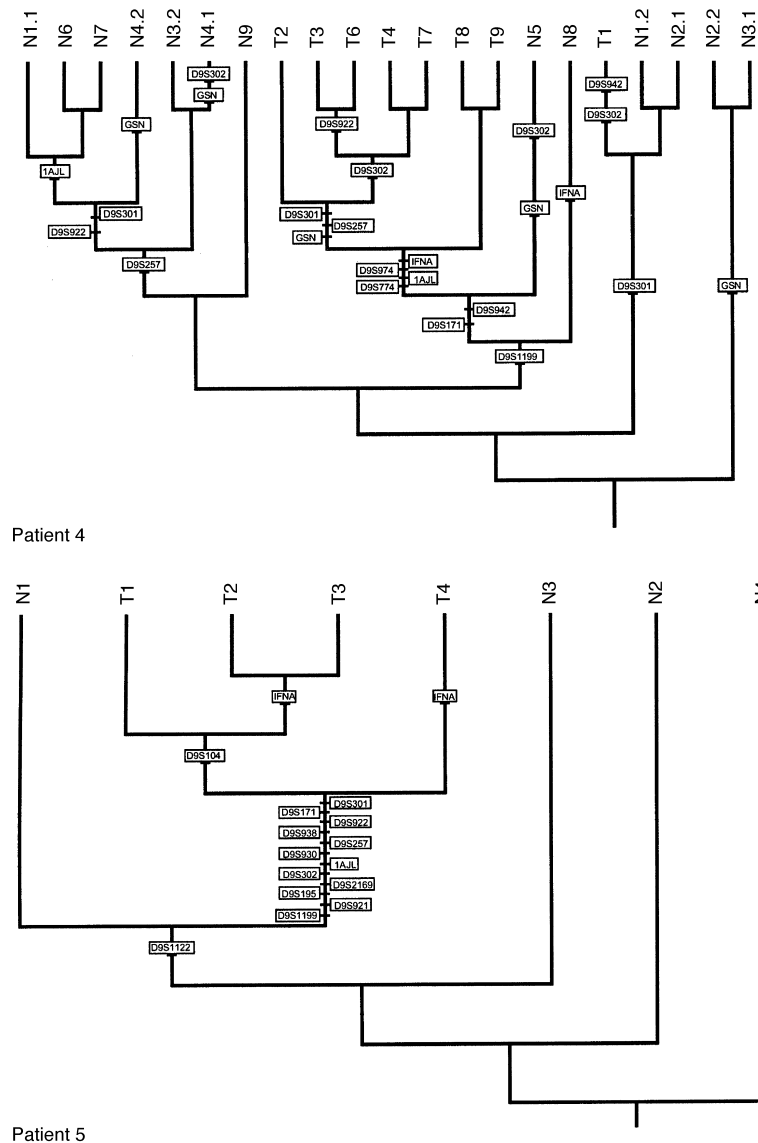


Fig. 8. The results of the phylogenetic analysis of patients 4 and 5 using individual microsatellite markers. These data were used for the ordering of tumours.

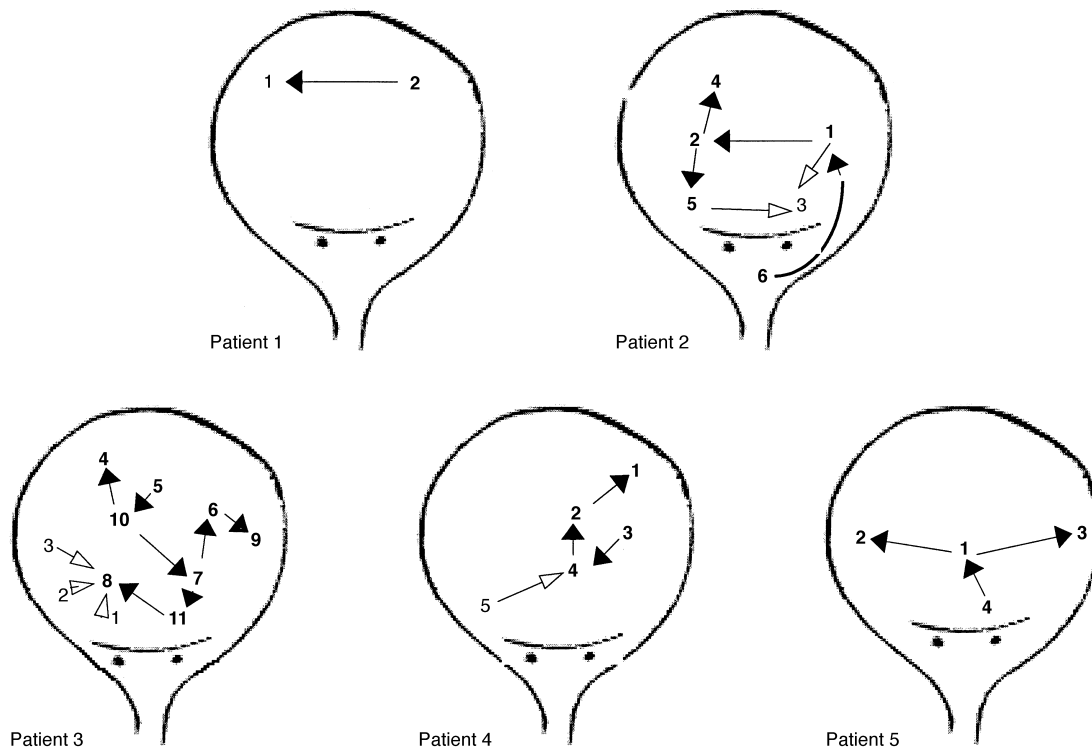


Fig. 9. Location of tumours for patients 1–5 with hypothetical progression models. The numbers are the sample codes listed in Table 1/Fig. 3. Arrows indicate the progression from the earliest tumours to the latest. Hatched arrows indicate the ambiguity.

## References

- Saran KK, Gould D, Godec CJ, Verma RS. Genetics of bladder cancer. *J Mol Med* 1996, **74**, 441–445.
- Richter J, Jiang F, Gorog JP, et al. Marked genetic differences between stage pTa and stage pT1 papillary bladder cancer detected by comparative genomic hybridization. *Cancer Res* 1997, **57**, 2860–2864.
- Ozen H. Bladder cancer. *Curr Opin Oncol* 1998, **10**, 273–278.
- Knowles MA. Identification of novel bladder tumour suppressor genes. *Electrophoresis* 1999, **20**, 269–279.
- Cairns P, Tokino K, Eby Y, Sidransky D. Homozygous deletions of 9p21 in primary human bladder tumors detected by comparative multiplex polymerase chain reaction. *Cancer Res* 1994, **54**, 1422–1424.
- Devlin J, Keen AJ, Knowles MA. Homozygous deletion mapping at 9p21 in bladder carcinoma defines a critical region within 2cM of IFNA. *Oncogene* 1994, **9**, 2757–2760.
- Packham JP, Taylor JA, Anna CH, White CM, Devereux TR. Homozygous deletions but no sequence mutations in coding regions of p15 or p16 in human primary bladder tumors. *Mol Carcinogenesis* 1995, **14**, 147–151.
- Orlow I, Lacombe L, Hannon GJ, et al. Deletion of the p16 and p15 genes in human bladder tumors. *J Natl Cancer Inst* 1995, **87**, 1524–1529.
- Williamson MP, Elder PA, Shaw ME, Devlin J, Knowles MA. p16 (CDKN2) is a major deletion target at 9p21 in bladder cancer. *Hum Mol Genet* 1995, **4**, 1569–1577.
- Torti FM, Lum BL. The biology and treatment of superficial bladder cancer. *J Clin Oncol* 1984, **2**, 505–531.
- Baud E, Catilina P, Boiteux JP, Bignon YJ. Human bladder cancers and normal bladder mucosa present the same hot spot of heterozygous chromosome-9 deletion. *Int J Cancer* 1998, **77**, 821–824.
- Hartmann A, Moser K, Kriegmair M, Hofstetter A, Hofstaedter F, Knuechel R. Frequent genetic alterations in simple urothelial hyperplasias of the bladder in patients with papillary urothelial carcinoma. *Am J Pathol* 1999, **154**, 721–727.
- Chaturvedi V, Li L, Hodges S, et al. Superimposed histologic and genetic mapping of chromosome 17 alterations in human urinary bladder neoplasia. *Oncogene* 1997, **14**, 2059–2070.
- Louhelainen J, Wijkström H, Hemminki K. Allelic losses demonstrate monoclonality of multifocal bladder tumors. *Int J Cancer* 2000, in press.
- Louhelainen J, Szyfter K, Szyfter W, Hemminki K. Loss of heterozygosity and microsatellite instability in larynx cancer. *Int J Oncol* 1997, **10**, 247–252.
- Louhelainen J, Lindstrom E, Hemminki K, Toftgard R. Dinucleotide repeat polymorphism within the tumor suppressor gene PTCH at 9q22. *Clin Genet* 1998, **54**, 239–241.
- de Nooij-van Dalen AG, van Buuren-van Seggelen VH, Lohman PH, Giphart-Gassler M. Chromosome loss with concomitant duplication and recombination both contribute most to loss of heterozygosity *in vitro*. *Genes Chromosomes Cancer* 1998, **21**, 30–38.
- Spruck CH 3rd, Ohneseit PF, Gonzalez-Zulueta M, et al. Two molecular pathways to transitional cell carcinoma of the bladder. *Cancer Res* 1994, **54**, 784–788.
- Shibata D, Navidi W, Salovaara R, Li ZH, Aaltonen LA. Somatic microsatellite mutations as molecular tumor clocks. *Nat Med* 1996, **2**, 676–681.
- Takahashi T, Habuchi T, Kakehi Y, et al. Clonal and chronological genetic analysis of multifocal cancers of the bladder and upper urinary tract. *Cancer Res* 1998, **58**, 5835–5841.
- Kerangueven F, Noguchi T, Coulier F, et al. Genome-wide search for loss of heterozygosity shows extensive genetic diversity of human breast carcinomas. *Cancer Res* 1997, **57**, 5469–5474.

22. Maddison WP, Maddison DR. Interactive analysis of phylogeny and character evolution using the computer program MacClade. *Folia Primatol* 1989, **53**, 190–202.
23. Swofford DL. *PAUP\*: Phylogenetic Analysis Using Parsimony (\* and other methods)*. Sunderland, Massachusetts, Sinauer Associates, 1999.
24. Gibas Z, Prout GR Jr, Connolly JG, Pontes JE, Sandberg AA. Nonrandom chromosomal changes in transitional cell carcinoma of the bladder. *Cancer Res* 1984, **44**, 1257–1264.
25. Sandberg AA, Berger CS, Haddad FS, Kerr D, Hecht F. Chromosome change in transitional cell carcinoma of ureter. *Cancer Genet Cytogenet* 1986, **19**, 335–340.
26. Berger CS, Sandberg AA, Todd IA, et al. Chromosomes in kidney, ureter, and bladder cancer. *Cancer Genet Cytogenet* 1986, **23**, 1–24.
27. Smeets W, Pauwels R, Laarakkers L, Debruyne F, Geraedts J. Chromosomal analysis of bladder cancer. III. Nonrandom alterations. *Cancer Genet Cytogenet* 1987, **29**, 29–41.
28. Van Tilborg AA, Hekman AC, Vissers KJ, van der Kwast TH, Zwarthoff EC. Loss of heterozygosity on chromosome 9 and loss of chromosome 9 copy number are separate events in the pathogenesis of transitional cell carcinoma of the bladder. *Int J Cancer* 1998, **75**, 9–14.
29. Tsai YC, Nichols PW, Hiti AL, Williams Z, Skinner DG, Jones PA. Allelic losses of chromosomes 9, 11, and 17 in human bladder cancer. *Cancer Res* 1990, **50**, 44–47.
30. Olumi AF, Tsai YC, Nichols PW, et al. Allelic loss of chromosome 17p distinguishes high grade from low grade transitional cell carcinomas of the bladder. *Cancer Res* 1990, **50**, 7081–7083.
31. Cairns P, Shaw ME, Knowles MA. Initiation of bladder cancer may involve deletion of a tumour-suppressor gene on chromosome 9. *Oncogene* 1993, **8**, 1083–1085.
32. Miyao N, Tsai YC, Lerner SP, et al. Role of chromosome 9 in human bladder cancer. *Cancer Res* 1993, **53**, 4066–4070.
33. Cairns P, Shaw ME, Knowles MA. Preliminary mapping of the deleted region of chromosome 9 in bladder cancer. *Cancer Res* 1993, **53**, 1230–1232.
34. Keen AJ, Knowles MA. Definition of two regions of deletion on chromosome 9 in carcinoma of the bladder. *Oncogene* 1994, **9**, 2083–2088.
35. Orlow I, Lianes P, Lacombe L, Dalbagni G, Reuter VE, Cordon-Cardo C. Chromosome 9 allelic losses and microsatellite alterations in human bladder tumors. *Cancer Res* 1994, **54**, 2848–2851.
36. Ruppert JM, Tokino K, Sidransky D. Evidence for two bladder cancer suppressor loci on human chromosome 9. *Cancer Res* 1993, **53**, 5093–5095.
37. Wu Q, Possati L, Montesi M, et al. Growth arrest and suppression of tumorigenicity of bladder-carcinoma cell lines induced by the P16/CDKN2 (p16INK4A, MTS1) gene and other loci on human chromosome 9. *Int J Cancer* 1996, **65**, 840–846.
38. Povey S, Attwood J, Chadwick B, et al. Report on the Fifth International Workshop on Chromosome 9 held at Eynsham, Oxfordshire, UK, 4–6 September 1996. *Ann Hum Genet* 1997, **61**, 183–206.
39. Simoneau M, Aboulkassim TO, LaRue H, Rousseau F, Fradet Y. Four tumour suppressor loci on chromosome 9q in bladder cancer: evidence for two novel candidate regions at 9q22.3 and 9q31. *Oncogene* 1999, **18**, 157–163.
40. Habuchi T, Yoshida O, Knowles MA. A novel candidate tumour suppressor locus at 9q32–33 in bladder cancer: localization of the candidate region within a single 840 kb YAC. *Hum Mol Genet* 1997, **6**, 913–919.
41. Habuchi T, Luscombe M, Elder PA, Knowles MA. Structure and methylation-based silencing of a gene (DBCCR1) within a candidate bladder cancer tumor suppressor region at 9q32–q33. *Genomics* 1998, **48**, 277–288.
42. Simoneau AR, Spruck CH 3rd, Gonzalez-Zulueta M, et al. Evidence for two tumor suppressor loci associated with proximal chromosome 9p to q and distal chromosome 9q in bladder cancer and the initial screening for GAS1 and PTC mutations. *Cancer Res* 1996, **56**, 5039–5043.
43. Czerniak B, Chaturvedi V, Li L, et al. Superimposed histologic and genetic mapping of chromosome 9 in progression of human urinary bladder neoplasia: implications for a genetic model of multistep urothelial carcinogenesis and early detection of urinary bladder cancer. *Oncogene* 1999, **18**, 1185–1196.
44. Richards FM, Goudie DR, Cooper WN, et al. Mapping the multiple self-healing squamous epithelioma (MSSE) gene and investigation of xeroderma pigmentosum group A (XPA) and PATCHED (PTCH) as candidate genes. *Hum Genet* 1997, **101**, 317–322.